Geol. Mag. **147** (*2*), *2010, pp. 233–241.* © *Cambridge University Press 2009*
doi:10.1017/S0016756809990641

HingeInflex: a MATLAB-based method for precise selection of the hinge and the inflection points in folds

DEEPAK C. SRIVASTAVA* & VIPUL RASTOGI†

*Department of Earth Sciences, Indian Institute of Technology Roorkee, Roorkee 247 667, Uttarakhand, India
†Department of Physics, Indian Institute of Technology Roorkee, Roorkee 247 667, Uttarakhand, India

(*Received* 27 January 2009; *accepted* 14 August 2009; First published online 30 October 2009)

Abstract – Subjectivity in visual selection of hinge and inflection points leads to significant errors in analyses of fold shapes in profile sections. This article gives a method for precise determination of these points. The method: (1) imports a fold image into MATLAB, (2) digitizes points on the image, (3) increases the number of available points by using an interpolation algorithm, (4) fits a polynomial curve to the points, and (5) searches for the hinge and the inflection points mathematically. Tests on several folds confirm that the 'HingeInflex' is a rapid, robust and user-friendly method for precise selection of the hinge and inflection points.

Keywords: fold shape analysis, polynomial fitting, hinge point, inflection point, MATLAB.

1. Introduction

Structural geologists have long used fold shapes as indicators of the kinematic, dynamic and rheological behaviour of rocks during deformation (Biot, 1961; Hudleston & Lan, 1993; Lan & Hudleston, 1996). Fold shape studies are also crucial in exploration of ore and petroleum deposits that are commonly concentrated in zones of high curvature, that is, the hinge zones of folds. The great significance of folds, as well as their prolific occurrence in layered rock sequences, has been the source of motivation for development of a number of methods for fold shape analysis during the last four decades (De Sitter, 1958; Ramsay, 1967; Twiss, 1988; Lisle, 1994; Pearce *et al.* 2006; Lisle *et al.* 2006).

Identification of the hinge point, that is, the point of maximum curvature on a folded surface, is an essential requirement in several methods of fold shape analysis. Some of these methods also require selection of the inflection point, the point at which the curvature changes its sign and crosses zero. In practice, however, these points are routinely selected by a visual estimation. This article addresses the issue of errors in visual estimation of the hinge point and the inflection point, and proposes a user-friendly computer-based method for precise selection of these points on a fold profile.

2. Methods of fold shape analysis

Accuracy in selection of the hinge points and/or inflection points is important in the analysis of fold shapes on profile sections by two types of methods: (1) methods that analyse a folded layer that is bounded by the outer and inner arcs, and (2) those methods that analyse a single folded surface, that is, the trace of a folded surface on the profile section.

*Author for correspondence: dpkesfes@iitr.ernet.in

Methods of the first type use the difference between curvatures of the outer and inner arcs to distinguish several standard shapes of the fold layers, such as Class 1A, Class 1B, Class 1C, Class 2 or Class 3 folds, and in some instances, to estimate the strain that concentrates during flattening stages of folding (Ramsay, 1967, pp. 411–14). Several versions of these methods exist: the t_α'/α method of Ramsay (1967, p. 413), the ϕ_α/α method of Hudleston (1973), the 'inverse thickness' method of Lisle (1992, 1997), the 'retrodeformational method' of Srivastava & Shah (2006), the 'Wellman' and the 'Mohr circle methods' of Shah & Srivastava (2006), and the 'isogon rosette' method of Srivastava & Shah (2008). Of these, the t_α'/α method is used most commonly and application of this method requires the selection of hinge points on the inner and outer arcs.

Methods of the second type define the shape of a single folded surface using quantitative shape parameters, such as the ratio of two harmonic coefficients (Mertie, 1959; Ramsay & Huber, 1987, pp. 314–17). These methods analyse the shape of a single folded surface by using Fourier analysis (Stabler, 1968; Hudleston, 1973; Stowe, 1988), conic section analysis (Bastida, Aller & Bobillo-Ares, 1999; Aller *et al.* 2004) or Bézier curve analysis (Bézier, 1966, 1967; De Paor, 1996; Wojtal & Hughes, 2001; Srivastava & Lisle, 2004; Coelho, Passchier & Grasemann, 2005; Lisle *et al.* 2006). Of these, the Bézier curve method is the most rapid and easy to use (Srivastava & Lisle, 2004; Lisle *et al.* 2006).

3. Errors in visual estimation

3.a. Hinge points

We address the issue of errors in visual estimation of the hinge point with the help of two examples, one of a

single layer fold and the other of a single folded surface. The fold in each example is analysed by considering two alternative positions of the hinge point.

3.a.1. *Single layer fold*

We give a natural example of a folded layer to demonstrate that uncertainty in the selection of hinge point can lead to significantly different strain estimates (Fig. 1a). As the inner arc is relatively sharp-crested, its hinge point can be marked fairly easily by visual estimation (point *3* in Fig. 1a). In contrast, the curvature distribution on the broad hinge zone of the outer arc is such that there is an uncertainty in the selection of a precise hinge point by visual estimation. Two possible and alternative positions of the hinge point, *1* and *2* are marked on the outer arc by visual estimation (Fig. 1a).

To demonstrate the importance of precision in selecting the hinge point, we analyse the fold in Figure 1a by the t_α'/α method, first by considering line *1–3* as the axial trace and then by considering line *2–3* as the axial trace (Fig. 1b, c). At low angles of limb dip ($\leq 20^\circ$), the left limb shows Class 1A geometry if line *1–3* is the axial trace (Fig. 1d). If, however, line *2–3* is the axial trace, then the same limb shows Class 1C geometry irrespective of the angle of limb dip (Fig. 1e). Although the right limb shows Class 1C geometry with respect to both the axial traces, the t_α'/α plots for this limb imply a significantly higher estimate of flattening strain if line *2–3*, rather line *1–3*, represents the axial trace (Fig. 1d, e). This example demonstrates that the results of shape analysis and estimates of flattening strain could be significantly different depending upon the choice of the hinge point or the axial trace.

The above example shows only one of several possible effects of the error in selection of the hinge point. For the sake of simplicity and application of the t_α'/α method, it assumes that tangents at the inner and outer arcs are parallel irrespective of whether the axial trace is *1–3* or *2–3*. In a strict sense, however, the tangents at the hinge points of the outer and inner arcs could parallel each other in only one of these two situations. A slight error in the selection of the hinge point on a sharp-crested arc results in a significant difference in the slope of the tangent at the hinge point, and no estimates of strain can be obtained if the tangents at the outer and inner arcs are non-parallel (Hudleston, 1973).

3.a.2. *Single folded surface*

Srivastava & Lisle (2004) and Aller *et al.* (2004) point out that subjectivity in the selection of the hinge point and the inflection point can be a potential source of error in fold shape analysis. In this article, we present an example to illustrate the issue of error in the visual estimation of the hinge point on a single folded surface (Fig. 2). Let us consider the profile section of a single folded surface and mark two possible hinge points, *1* and *2*, by visual estimation (inset in Fig. 2). The analysis of this fold by the Bézier curve method reveals that a small difference in position of the hinge point leads to significant differences in the shape parameter as well as the aspect ratio of the fold (Fig. 2).

3.b. Inflection points

The uncertainty in the visual estimation of inflection points is also a potential source of error in the shape analysis of single folded surfaces. The inset in Figure 3a is an example of a folded surface on which two possible positions of the inflection points, i_1 and i_2 are marked by visual estimation. The analysis of this fold using the Bézier curve method yields significantly different values of the shape parameter and the aspect ratio depending upon the choice of the inflection point (Fig. 3b).

4. Precise selection of the hinge and the inflection points

4.a. The algorithm

The curvature $C(x)$ at any point (x, y) on the profile section of a folded surface, $y = f(x)$, is given by (Ramsay, 1967, p. 347):

$$C(x) = \frac{\dfrac{d^2y}{dx^2}}{\left(1 + \left(\dfrac{dy}{dx}\right)^2\right)^{3/2}} \qquad (1)$$

The algorithm calculates the derivatives dy/dx and d^2y/dx^2 and substitutes these values in Eq. 1 to determine the curvature $C(x)$ at different points (x, y) on the fold. The method produces a curvature distribution curve for selection of the point $(x_{\max}, y_{\max})$ where curvature $C(x)$ attains the maximum value, and the point $(x_{\inf}, y_{\inf})$ where it changes its sign and crosses zero.

Four potential sources of error are implicit in our approach. First, any irregularity on the fold limb may appear as a spurious hinge point due to an anomalously high curvature. Our method obviates appearance of such erroneous hinge points by fitting a smooth n^{th} degree polynomial curve, $y = a_n x^n + a_{n-1}x^{n-1} + \cdots + ax + a_0$, on the given fold.

Second, the accuracy in selection of the hinge point critically depends upon the smoothness of the curve that connects the successive points on the fold profile (Fig. 4a). The nature of curvature distribution with respect to the manually digitized points is, however, commonly uneven in natural folds (Fig. 4b). By best-fitting a polynomial curve through points on the fold, we obtain a curvature distribution curve that is smooth enough for precise selection of the hinge and inflection points (Fig. 4c, d).

Third, the precision in the results also depends upon the accuracy in curve-fitting. One simple way to improve the accuracy is to use a large number of points on the fold profile. Extraction of more than 100 points on a mesoscopic-scale folded surface is,

https://doi.org/10.1017/S0016756809990641 Published online by Cambridge University Press

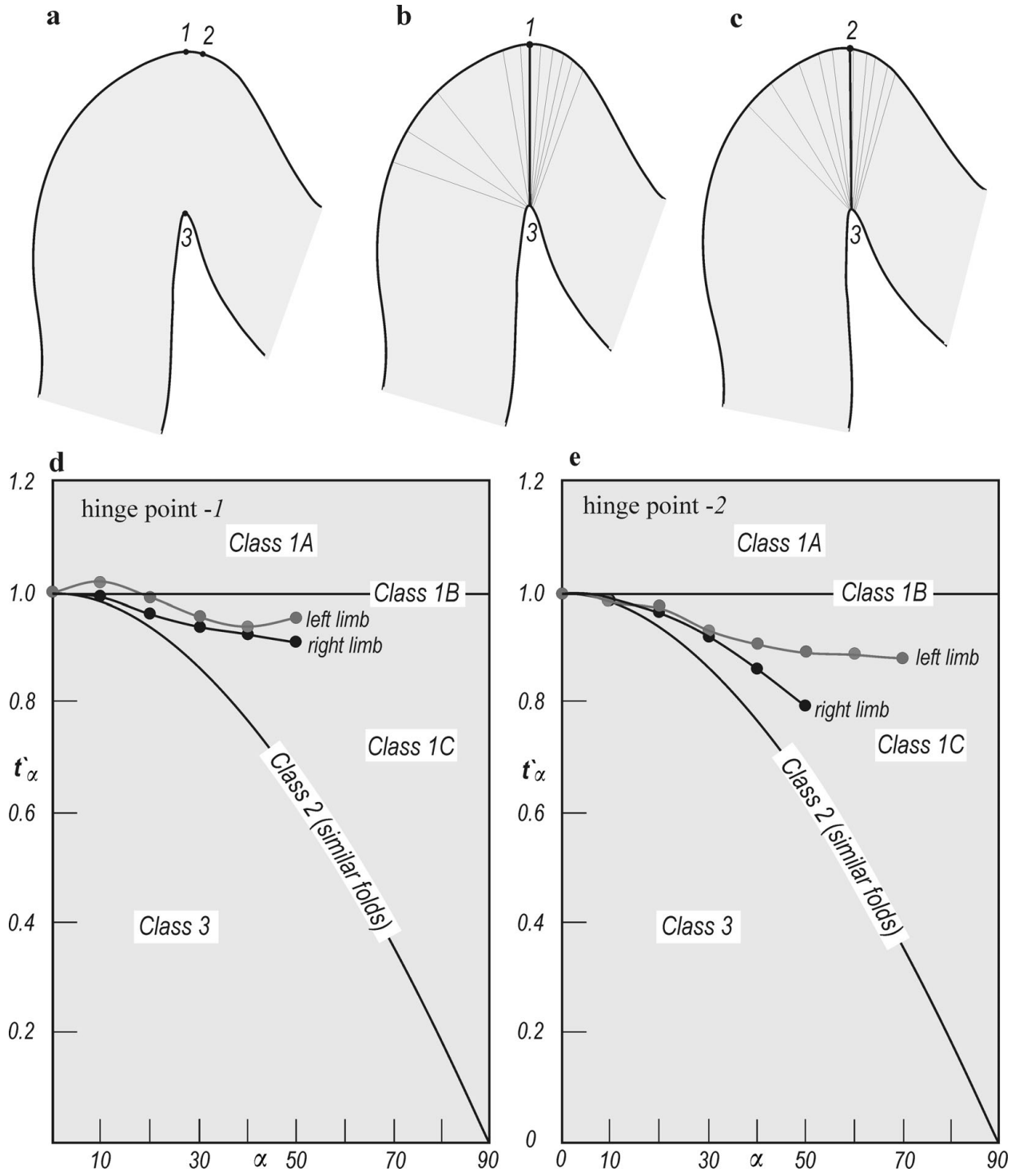

Figure 1. Effect of uncertainty in visual selection of the hinge point on a single layer fold. (a) Profile section of a fold in the Almora crystalline, Kumaun Lesser Himalaya. *1* and *2* – two alternative positions of the hinge point on the outer arc, *3* – hinge point on the inner arc. (b, c) Isogon patterns with respect to axial traces *1–3* and *2–3*, respectively. The isogons on left limb are more convergent in (b) as compared to those in (c). (d, e) t'_α /α plots with respect to the axial traces *1–3* and *2–3*, respectively. Curves in (d) and (e) indicate different shapes and estimates of flattening.

however, quite time-intensive. Our method overcomes this limitation by using the interpolation technique that generates several intermediate points between the digitized data points. Typically, the interpolation increases the number of points from 100 to 500–1000.

Finally, the curvature analysis in some folds may report false hinge and inflection points even after best-fitting the smooth polynomial curve and increasing the points by interpolation. The false points correspond to unavoidable sharp turns that occur towards the end points of the high degree polynomial fitted to the fold. Our method excludes the sharp turns by delimiting the search domain to a small segment of the polynomial curve that is likely to contain the hinge

https://doi.org/10.1017/S0016756809990641 Published online by Cambridge University Press

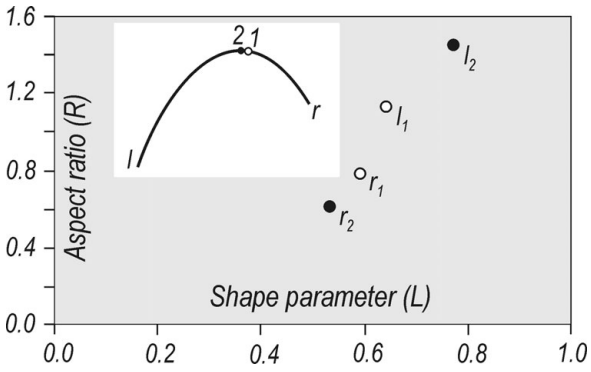

Figure 2. Effect of uncertainty in visual selection of the hinge point on a single folded surface. Inset shows a folded surface with two alternative positions, *1* and *2*, of the hinge point. *l* and *r* – left and right limbs. The graph shows results of shape analysis by the Bézier curve method. l_1, r_1 and l_2, r_2 – shapes of left and right limbs with respect to hinge points *1* and *2*, respectively. Aspect ratio (R) – amplitude/quarter wavelength; Shape parameter (L) – length of Bézier handle/quarter wavelength (for details see Srivastava & Lisle, 2004).

point. Similarly, another segment of the curve may be selected for searching the inflection point. The flexibility of choosing a segment of the fold facilitates piecewise analysis of the fold.

Figure 4c represents an example where the polynomial fitting results in a sharp turn towards the edge of left limb of the fold. We obviate the sharp turn by selecting a potential segment that is likely to contain the hinge point. Similarly, we select a potential segment containing a single zero crossing for searching the inflection point on the right limb. This selection of a potential segment also obviates the zero crossing towards the edge of right limb, possibly an artifact of polynomial fitting and numerical differentiation. The code can mark multiple inflection points within the chosen segment and this feature can be utilized to analyse the folds with multiple hinge points or the parasitic folds.

4.b. 'HingeInflex'

The MATLAB code, namely, 'HingeInflex' (online Appendix at http://journals.cambridge.org/geo), imports the image of a fold profile, digitizes different points on the image, increases the number of points by interpolation and fits a smooth polynomial curve through the points. It calculates the first derivative and the second derivative at each point on the polynomial, substitutes these values in Eq. (1) and determines the values of curvature at different points.

We have used the cubic spline smoothing method for interpolating the digitized data points, least-squares fitting procedure for polynomial fitting and numerical differentiation for determining derivatives at different points on the fold. The degree of best-fitted polynomial has been determined by minimizing the residuals.

The step-by-step procedure for selection of the hinge point and the inflection point is as follows:

(1) Import the image of the given fold profile into MATLAB and digitize it by using any commonly available software, such as the free program 'GRABIT' (J. Doke, unpub. data, 2005; http://www.mathworks.com/matlabcentral/fileexchange/7173).

(2) Extract and store the co-ordinates (x, y) of all the points in a MATLAB data file. The code prompts for the file selection menu. Use the menu to load the data file and plot the digitized data points (Fig. 5a).

(3) Obtain the best-fit curve through the points by using the provisions, given in the code, for fitting a polynomial curve and for changing the degree of polynomial. This operation produces a single smooth curve through the extracted data points.

The code prompts for polynomial fitting and asks for the degree of polynomial. It fits the polynomial of chosen degree and displays the fitted curve through the data points (Fig. 5a). It also calculates and displays the residuals at different points. By changing the degree of the polynomial, the user obtains the best-fit that

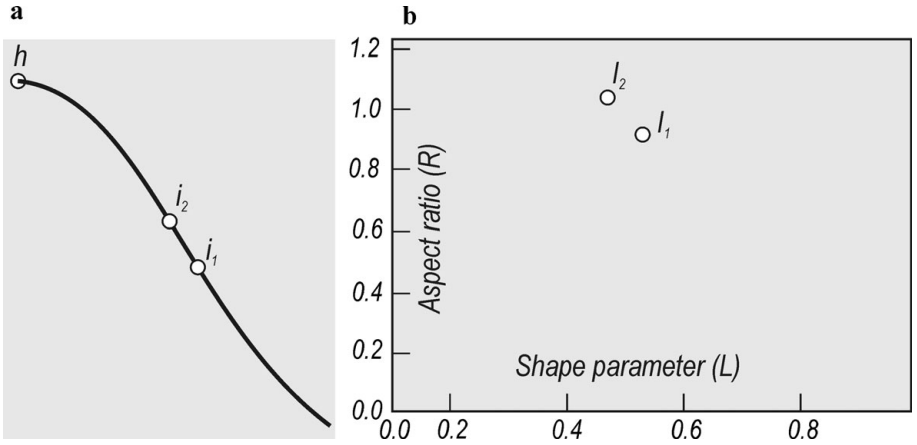

Figure 3. Effect of uncertainty in visual selection of the inflection point. (a) h – hinge point, i_1 & i_2 – two alternative positions of the inflection point on a fold limb. (b) Results of shape analysis of the fold limb by the Bézier curve method. I_1 and I_2 – shapes of the fold limb with respect to the inflection points i_1 and i_2, respectively. Aspect ratio (R) and Shape parameter (L) same as in Figure 2.

https://doi.org/10.1017/S0016756809990641 Published online by Cambridge University Press

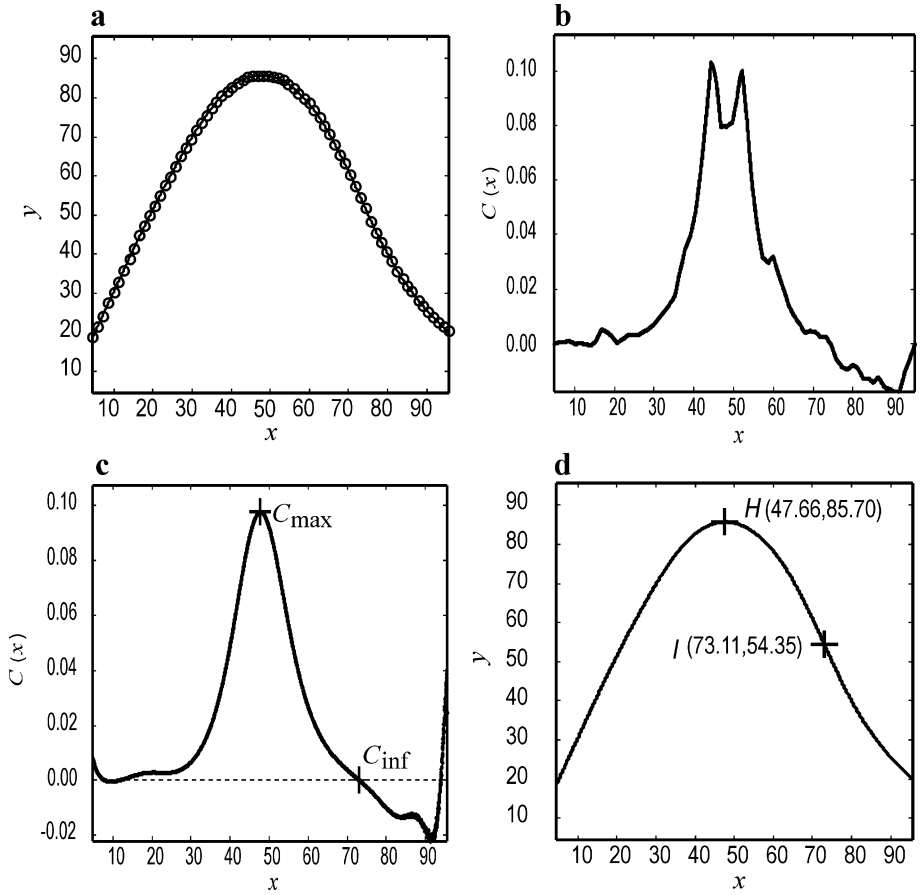

Figure 4. (a) Digitized points on an image of the fold profile. (b) Irregular nature of curvature distribution. No polynomial curve is fit to the digitized points. (c) Smooth curvature distribution obtained by fitting a polynomial of degree 14 to the digitized data points. $C(x)$ – curvature, C_{max} – the point of maximum curvature, C_{inf} – the point where the curvature changes sign and crosses zero. (d) Hinge point H and inflection point I on the fold.

corresponds to the minimum value of the residuals (Fig. 5b).

The code calculates curvature $C(x)$ at a large number of points on the fitted polynomial curve and gives the curvature distribution curve that shows variation in $C(x)$ with respect to x (Fig. 5c).

(4) By using the provision in the code, select two potential segments of the curvature distribution curve, one containing the hinge point and the other containing the inflection point(s). The code searches for the point C_{max} where $C(x)$ attains the maximum and for the point(s) C_{inf} where it crosses zero, and marks these points on the curvature distribution curve (Fig. 5c). Finally, it marks the points corresponding to C_{max} and C_{inf} as the hinge point H and the inflection point(s) I on the fold (Fig. 5d).

Fitting a polynomial curve in step (3) is difficult on overturned folds that have two or more points with different values of y for a single value of x (Fig. 6a). Such folds require an additional step between step (2) and step (3) given above. The additional step rotates the digitized image through an arbitrary angle such that every point on the fold has a unique value of y (Fig. 6b). A polynomial curve can now be easily fitted to the digitized points on the rotated fold image (Fig. 6c). The rotation also facilitates fitting of a polynomial curve to those folds in which the tangent at the hinge point is not horizontal.

5. Examples

We have tested our code on a large number of natural and graphically-simulated folds. Here we list three examples: (1) an open asymmetric fold that has a broad hinge zone (Fig. 5a), (2) an overturned asymmetric fold with relatively narrow hinge zone (Fig. 6a) and (3) a natural cuspate fold (Fig. 7a, traced from a part of figure 17.4 in Ramsay & Huber, 1987, p. 350).

Visual estimation of the hinge point of the fold in Figure 5a involves uncertainty due to the nature of curvature distribution on the broad hinge zone. The proposed method generates 500 points by cubic smoothing spline interpolation to the digitized data points and fits a polynomial of degree 9. These operations facilitate fitting a single smooth curve through the points (Fig. 5a). The quality of fitting is ensured by monitoring and minimizing the residuals (Fig. 5b). The distinct peak C_{max} and the zero-crossing C_{inf} in the curvature distribution plot (Fig. 5c) correspond to the hinge point H and the inflection point I on the fold profile (Fig. 5d).

https://doi.org/10.1017/S0016756809990641 Published online by Cambridge University Press

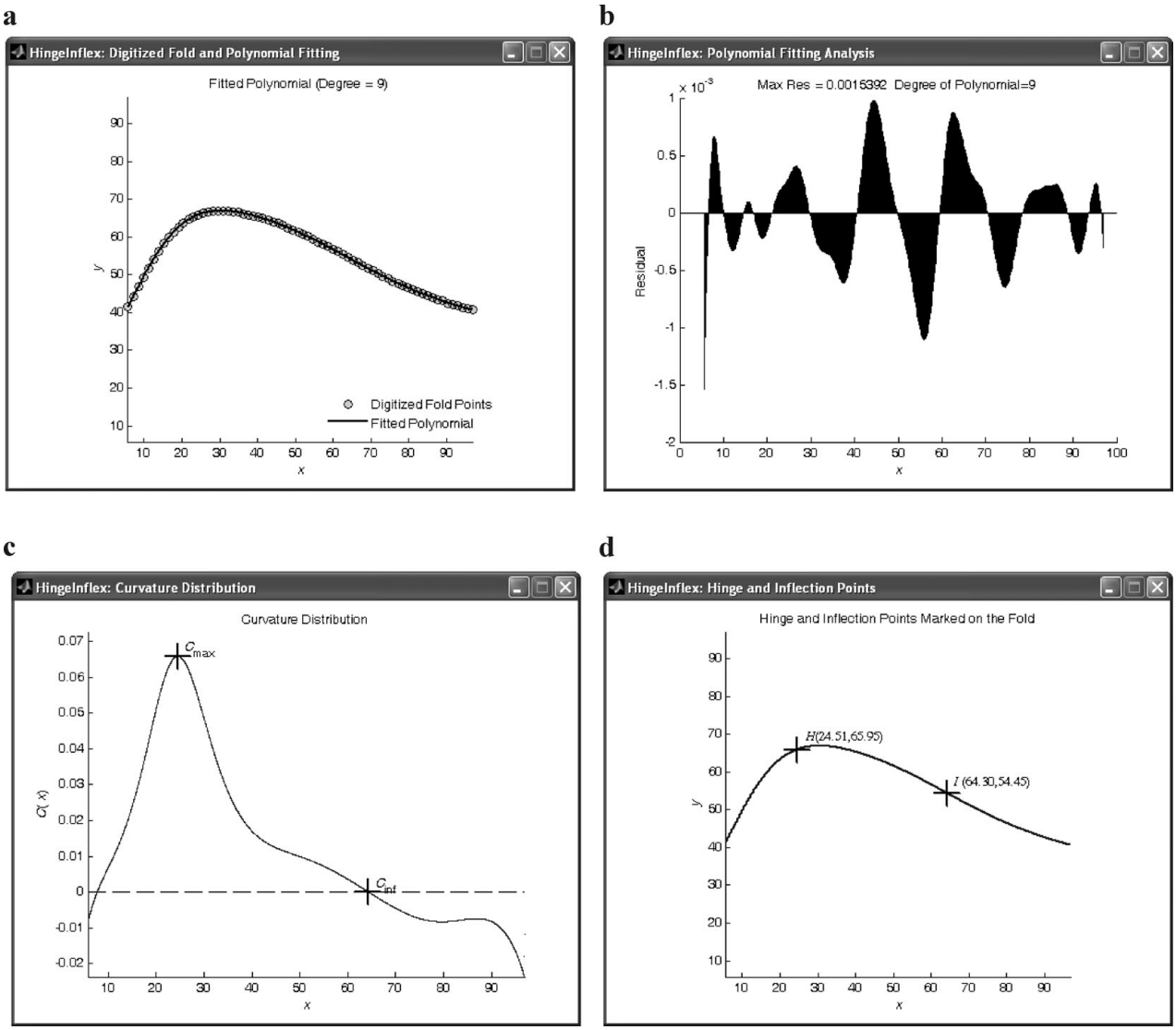

Figure 5. (a) Digitized data points and the best-fitted polynomial on an asymmetric fold. (b) Residuals at different points on the fold. (c) Curvature distribution curve showing the maximum curvature point C_{max} and the zero crossing point C_{inf}. (d) Precise positions of hinge point H and inflection point I on the fold.

The overturned asymmetric fold in Figure 6a is an example of a curve on which a few points have a common value of x but different values of y. In order to fit a polynomial curve to such a fold, it is necessary to rotate the fold image prior to the fitting (Fig. 6b). Figure 6c shows the digitized data points on the image, rotated through an angle of 33°, along with the smooth fitted polynomial of degree 17. The small values of residuals as shown in Figure 6d indicate the satisfactory curve fitting. The curvature $C(x)$ can now be calculated (Fig. 6e) to search for precise positions of the hinge and inflection points (H and I in Fig. 6f).

Figure 7a is an example of a natural cuspate fold and Figure 7b shows the digitized data points on this fold. We have rotated the fold by 10° to facilitate polynomial curve fitting (Fig. 7c). Small values of residuals at different points on the curve indicate satisfactory curve fitting (Fig. 7d). The curvature distribution curve shows the peak C_{max} and the zero crossings C_{inf} corresponding to the hinge point H and the inflection points I, respectively (Fig. 7e). These points are also marked on the fold (Fig. 7f).

6. Summary and conclusions

The shape analysis of folds is sensitive to a lack of precision in the selection of the hinge and inflection points. 'HingeInflex' is a user-friendly method for the mathematical determination of these points on those folds that can be fitted with a smooth polynomial curve. We give a MATLAB code that best-fits a smooth polynomial curve and selects the hinge and the inflection points by calculating and comparing the curvature at different points of the curve.

The method has an in-built flexibility for changing the degree of polynomial curve and ensuring the best-fit by monitoring and minimizing the residuals. It also provides an option to delimit the potential search domain for obviating the appearance of spurious hinge or inflection points and obtaining the rapid results. Tests

https://doi.org/10.1017/S0016756809990641 Published online by Cambridge University Press

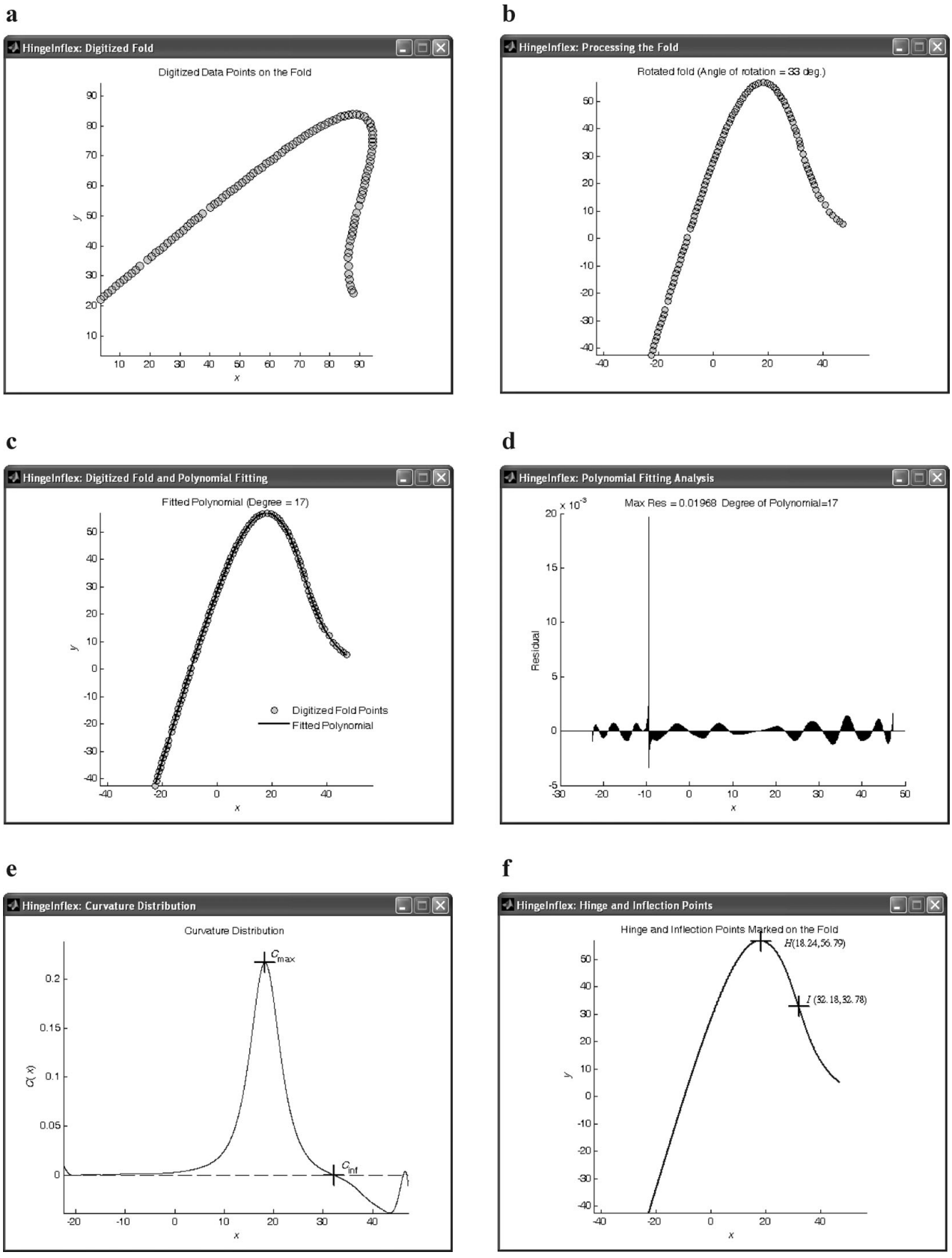

Figure 6. (a) Digitized data points on the image of an overturned fold. Several points on the right limb have same value of x but different values of y. (b) Rotated image of fold in (a). (c) Best-fitted polynomial through digitized points on fold in (b). (d) Distribution of residuals along the fold. (e) Curvature distribution with the maximum curvature point at C_{max} and the zero crossing point at C_{inf}. (f) Hinge point H and inflection point I on the fold.

https://doi.org/10.1017/S0016756809990641 Published online by Cambridge University Press

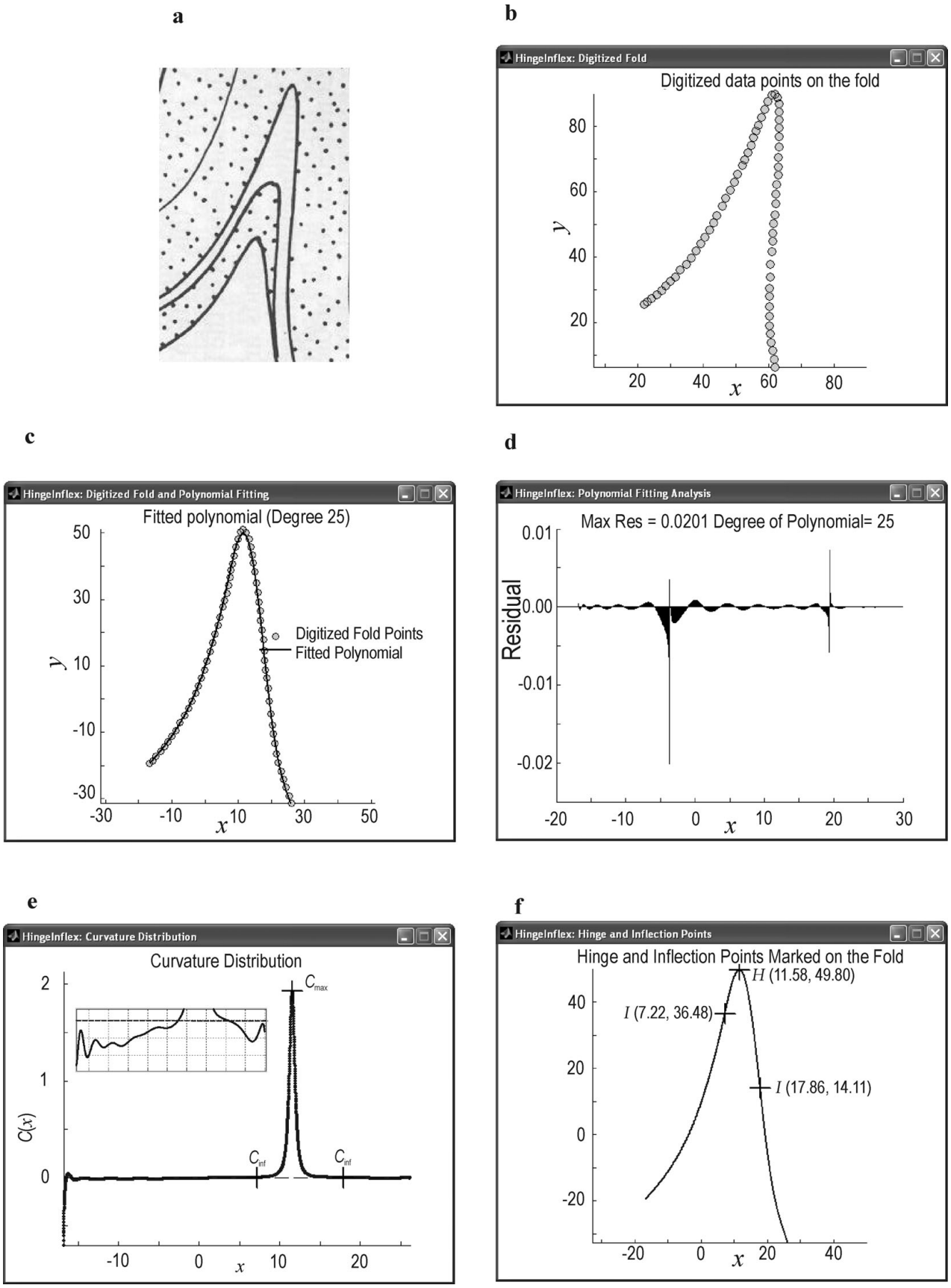

Figure 7. (a) Natural example of a cuspate fold (part of figure 17.4 in Ramsay & Huber, 1987, p. 350). (b) Digitized data points on the fold. (c) Rotation of data points in (b) by 10° and the best-fit polynomial through the data points. (d) Residual distribution along the fold. (e) Curvature distribution showing the maximum curvature point C_{max} and the zero crossing points C_{inf}. Inset shows the magnified distribution around zero axis. (f) Inflection points I and the hinge point H are marked on the fold.

https://doi.org/10.1017/S0016756809990641 Published online by Cambridge University Press

on several natural and computer-simulated folds reveal that 'HingeInflex' is a robust method that accurately identifies positions of hinge and inflection points.

Acknowledgements. Jyoti Shah, Dipanwita Nandi, Alisha Mehra and Rajit Ghosh tested our method on several examples of computer simulated and natural folds. We are grateful to an anonymous referee, Richard Lisle and Richard Jones for erudite reviews and to the Earth Science System Division of Department of Science and Technology, Government of India, for the funding.

References

ALLER, J., BASTIDA, F., TOIMIL, N. C. & BOBILLO-ARES, N. C. 2004. The use of conic sections for the geometrical analysis of folded profile surfaces. *Tectonophysics* **379**, 239–54.

BASTIDA, F., ALLER, J. & BOBILLO-ARES, N. C. 1999. Geometrical analysis of surfaces using simple functions. *Journal of Structural Geology* **21**, 729–42.

BÉZIER, P. 1966. Définition numérique de courbes et surfaces, part 1. *Automatisme* **11**, 625–32.

BÉZIER, P. 1967. Définition numérique de courbes et surfaces, part 2. *Automatisme* **12**, 17–21.

BIOT, M. A. 1961. Theory of folding of stratified viscoelastic media and its implication in tectonics and orogenesis. *Geological Society of America Bulletin* **72**, 1595–1620.

COELHO, S., PASSCHIER, C. & GRASEMANN, B. 2005. Geometric description of flanking structures. *Journal of Structural Geology* **27**, 597–606.

DE PAOR, D. G. 1996. Bézier curves and geological design in structural geology and personal computers. In *Structural Geology and Personal Computers* (ed. D. G. De Paor), pp. 389–417. Oxford: Pergamon Press.

DE SITTER, L. U. 1958. Boudins and parasitic folds in relation to cleavage and folding. *Geologie en Mijnbouw* **20**, 272–86.

HUDLESTON, P. J. 1973. Fold morphology and some geometrical considerations of theories of fold development. *Tectonophysics* **16**, 1–46.

HUDLESTON, P. J. & LAN, L. 1993. Information from fold shapes. *Journal of Structural Geology* **15**, 253–64.

LAN, L. & HUDLESTON, P. J. 1996. Rock rheology and sharpness of folds in single layers. *Journal of Structural Geology* **18**, 925–31.

LISLE, R. J. 1992. Strain estimation from flattened buckle folds. *Journal of Structural Geology* **14**, 369–71.

LISLE, R. J. 1994. Detection of zones of abnormal strains in structures using Gaussian curvature analysis. *American Association of Petroleum Geologists Bulletin* **78**, 1811–19.

LISLE, R. J. 1997. A fold classification scheme based on a polar plot of inverse layer thickness. In *Evolution of Geological Structures in Micro- to Macro-Scales* (ed. S. Sengupta), pp. 323–39. London: Chapman and Hall.

LISLE, R. J., MARTÍNEZ, J. L. F., BOBILLO-ARES, N., MENÉNDEZ, O., ALLER, J. & BASTIDA, F. 2006. FOLD PROFILER: A MATLAB-based program for fold shape classification. *Computers & Geosciences* **32**, 102–8.

MERTIE, J. B. 1959. Classification, delineation and measurement of non-parallel folds. *U. S. Geological Survey, Professional Paper* **314-E**, 91–124.

PEARCE, M. A., JONES, R., SMITH, S. A. F., MCCAFFREY, K. J. W. & CLEGG, P. 2006. Numerical analysis of fold curvature using data acquired by high-precision GPS. *Journal of Structural Geology* **28**, 1640–6.

RAMSAY, J. G. 1967. *Folding and Fracturing of Rocks*. New York: McGraw-Hill, 568 pp.

RAMSAY, J. G. & HUBER, M. I. 1987. *The Techniques of Modern Structural Geology, Vol.* **2***: Folds and Fractures*. London: Academic Press Inc.

SHAH, J. & SRIVASTAVA, D. C. 2006. Strain estimation from flattened parallel folds: application of the Wellman method and Mohr circle. *Geological Magazine* **143**, 243–7.

SRIVASTAVA, D. C. & LISLE, R. J. 2004. Rapid analysis of fold shape using Bézier curves. *Journal of Structural Geology* **26**, 1553–9.

SRIVASTAVA, D. C. & SHAH, J. 2006. A rapid method for strain estimation from flattened parallel folds. *Journal of Structural Geology* **28**, 1–8.

SRIVASTAVA, D. C. & SHAH, J. 2008. The 'isogon rosette' method for rapid estimation of strain in flattened folds. *Journal of Structural Geology* **30**, 444–50.

STABLER, C. L. 1968. Simplified Fourier analysis of fold shapes. *Tectonophysics* **6**, 343–50.

STOWE, C. W. 1988. Application of Fourier analysis for computer representation of fold profiles. *Tectonophysics* **156**, 303–11.

TWISS, R. J. 1988. Description and classification of folds in single surfaces. *Journal of Structural Geology* **10**, 607–23.

WOJTAL, S. & HUGHES, G. 2001. Using Bézier curves to analyze the shapes of folded surfaces. *Abstracts with Program, Geological Society of America* **33**(6), 26.